*Molecular Vision* 2023; 29:306-316 <http://www.molvis.org/molvis/v29/306>
Received 9 May 2022 | Accepted 2 November 2023 | Published 6 November 2023



# Sulforaphane inhibits TGF-β-induced fibrogenesis and inflammation in human Tenon's fibroblasts

**Yang Liu,[1] Yangbin Huang,[1] Zihan Guo,[1] Chengcheng Yang,[1] Yunzepeng Li,[1] Binhui Li,[1] Ye Liu,[2] Hui Zheng[1]**

*[1]Department of Ophthalmology, the Fifth Affiliated Hospital, Sun Yat-sen University, Zhuhai, PR China; [2]Department of Pathology, the Fifth Affiliated Hospital, Sun Yat-sen University, Zhuhai, PR China*

**Purpose:** Subconjunctival fibrosis is the main cause of failure after glaucoma filtration surgery. We explored the effects of sulforaphane (SFN) on the conversion of human Tenon's fibroblasts (HTFs) into myofibroblasts, transforming growth factor (TGF)–β-induced contraction of collagen gel, and inflammation.

**Methods:** After treatment with the combination of TGF-β and SFN or TGF-β alone, primary HTFs were subjected to a three-dimensional collagen contraction experiment to examine their contractility. Levels of α smooth muscle actin (α-SMA), synthesis of extracellular matrix (ECM), and phosphorylation of various signaling molecules were determined by western blot or quantitative reverse transcription-polymerase chain reaction (RT-qPCR). Fluorescence microscopy was employed to examine stress fiber formation in HTFs. The expressions of interleukin (IL)-6, IL-8, and connective tissue growth factor (CTGF) were determined using RT-qPCR.

**Results:** The contraction of myofibroblasts caused by TGF-β was significantly suppressed by SFN. This suppressive effect was exerted via the differentiation of HTFs into myofibroblasts by inhibiting the production of fibronectin and the expression of α-SMA. Moreover, SFN treatment reduced the expression of TGF-β-promoted integrins β1 and α5, myosin light chain (MLC) phosphorylation, and stress fiber formation, as well as the expression of IL-6, IL-8, and CTGF. Finally, TGF-β-induced Smad2/3 and extracellular signal-regulated kinase (ERK) phosphorylations were attenuated by SFN.

**Conclusions:** SFN inhibits HTF contractility, differentiation into myofibroblasts, and inflammation caused by TGF-β. These effects are mediated by both classic and non-classic signaling pathways. Our results indicate that SFN has potent anti-fibrotic and anti-inflammatory effects in HTFs and is a potential candidate for subconjunctival fibrosis therapy.

Most cases of blindness worldwide are caused by glaucoma. According to existing evidence, 79.6 million individuals were affected by glaucoma globally in 2020 [1]. If laser surgery and medication are unable to control intraocular pressure, filtration surgery is the preferred choice of treatment for these patients. This surgical approach creates a functioning bleb that drains aqueous from the anterior chamber of the eye. An effective filtration bleb is key to maintaining intraocular pressure after the operation. Most failures after surgery are caused by the formation of scars and subconjunctival fibrosis at the filtering bleb site, and strategies for effective intervention are limited. Although the success rate of filtration surgeries has been observed to improve when antiproliferative agents such as mitomycin C and 5-fluorouracil are used during the surgery [2,3], these drugs have been connected to severe and potentially blinding complications [4]. Hence, improved therapeutic approaches with fewer side effects are urgently needed.

Correspondence to: Hui Zheng, Department of Opthalmology, Fifth Affiliated Hospital of Sun Yat-sen University, 52 Road Meihuadong, Zhuhai 519000, PR China. Phone: +86-756-252-8738; FAX: +86-756-252-8333. email: 13926927853@139.com

The formation of scars in the filtering bleb after glaucoma filtering surgery is a multifactorial process. Conjunctiva wound healing is an inflammation-mediated process, followed by fibroblast migration, proliferation, differentiation, extracellular matrix (ECM) synthesis, wound contraction, and subconjunctival fibrous scar formation [5]. As the major sources of myofibroblasts, human Tenon's fibroblasts (HTFs) can differentiate into myofibroblasts after stimulation with fibrogenic factors and are significantly connected to the pathogenesis of bleb scarring [6]. Among various growth factors, transforming growth factor (TGF)–β is significantly associated with failures caused by excessive subconjunctival fibrosis and inflammation after the glaucoma filtering surgery [7]. The interaction between TGF-β and its receptors can trigger Smad-dependent or -independent signaling cascades, such as Rho GTPase, phosphoinositide 3-kinase (PI3K)/Akt, and mitogen-activated protein kinase (MAPK) pathways [8,9]. Among the members of the MAPK family, both extracellular signal-regulated kinase (ERK) and p38/MAPK are activated by TGF-β. Akt is one of the major downstream intermediaries of the PI3K signaling pathway, and its activation by TGF-β regulates different physiologic processes [10]. Interestingly, TGF-β signaling pathway inhibition by

Rho-associated kinase inhibitor AR12286 was shown to reduce fibrosis after glaucoma filtration surgery [11]. Ceralasertib can inhibit TGF-β1-induced fibrotic response by regulating the PI3K/AKT pathway and checkpoint kinase 1/P53 [12]. Therefore, molecules associated with these pathways are potential candidates for anti-fibrotic therapy.

Sulforaphane (SFN) is a naturally occurring isothiocyanate derived from cruciferous vegetables, such as broccoli and cauliflower, presenting antioxidant, anti-inflammatory, cytoprotective, and anti-apoptotic effects achieved through regulating diverse molecular mechanisms [13,14]. Due to its suppressive effect on TGF-β activity, SFN can participate in anti-fibrotic processes. In hepatocellular carcinoma cells, SFN can significantly suppress the epithelial-mesenchymal transition (EMT) caused by TGF-β by regulating ROS-associated pathways [15]. Moreover, SFN can attenuate pulmonary fibrosis by inhibiting EMT via TGF-β/Smads signaling pathways [16]. However, the potential role of SFN in the contractility of HTFs is unclear. We explored the regulatory roles of SFN in myofibroblast differentiation and the contraction of collagen gel caused by TGF-β, as well as the expression of HTF-mediated inflammatory factors. Additionally, we analyzed how SFN regulates the expression of integrins and the phosphorylation of various signaling proteins in HTFs.

## METHODS

*Reagents:* Native porcine type I collagen was provided by Nitta Gelatin (Osaka, Japan), and fetal bovine serum (FBS) and Eagle's minimum essential medium (MEM) were obtained from Invitrogen-Gibco (Gibco). R&D Systems provided recombinant human TGF-β1 (Minneapolis, MN). Antibodies against Smad2/3, phospho-Smad2/3, ERK, p38, phospho-p-38, Akt, phospho-Akt, myosin light chain (MLC), and phospho-MLC were purchased from Cell Signaling Technology (Danvers, MA). Antibodies against glyceraldehyde 3-phosphate dehydrogenase (GAPDH) were provided by Proteintech (Rosemont, IL). Antibodies against α-SMA and SFN were provided by Sigma-Aldrich. Fibronectin was purchased from Abcam (Boston, MA). Beyotime (Shanghai, China) provided bovine serum albumin (BSA), enhanced chemiluminescence (ECL) reagents, horseradish peroxidase (HRP), and secondary antibodies. 4′,6-diamidino-2-phenylindole (DAPI) was purchased from MP Biomedicals (Irvine, CA), and rhodamine phalloidin was obtained from Cytoskeleton (Denver, CO). Cell Counting Kit-8 (CCK-8) was bought from Dojindo Molecular Technology (Kumamoto, Japan).

*Isolation and culture of HTFs:* The Ethics Committee of the Fifth Affiliated Hospital of Sun Yat-sen University reviewed and approved all the protocols and procedures employed in this study (Approval number: K89–1). HTFs were obtained from three individuals undergoing strabismus surgery after written informed consent forms were signed [17]. Subconjunctival tissues were collected to isolate the HTFs. All procedures strictly followed the Declaration of Helsinki. Three young Chinese patients, two male and one female, with ages ranging from 18 to 30 years, were identified as having no history of systemic or conjunctival diseases, and no prior use of topical ocular medications. After a 1-h digestion in collagenase (2 mg/ml) at 37°C, cell suspensions were cultured with MEM supplemented with 10% FBS for 3 to 7 passages before the beginning of the experiments. Morphological examination and cytokeratin and vimentin quantification were used to determine the purity of the cultured HTFs. Cells that exhibited negative cytokeratin and positive vimentin expression were used (data not shown).

*Collagen gel contraction assays:* Collagen gels were prepared as previously described [17]. Briefly, HTFs suspension ($1.1\times10^6$ cells/ml), 10×MEM, reconstitution buffer (0.2 M HEPES, 0.26 M $Na_2CO_3$, and 0.05 M NaOH pH [7.3]) and type I collagen (3 mg/ml) were mixed on ice in the volume ratio of 2:1:1:7. After 1 h of coating using 1% BSA at 37 °C, the mixture (0.5 ml) was added to each well of a 24-well plate. After the collagen gels solidified, they were separated from the well with a micro spatula, and serum-free MEM with or without SFN or TGF-β was added. Next, we determined the gel diameter, and the following formula was used to calculate the extent of contraction: gel contraction = (initial diameter)/(diameter at each time point).

*Cell viability assay:* The cell viability effect of the vehicle dimethylsulfoxide (DMSO) was evaluated using the CCK-8 assay. Specifically, HTFs were seeded at a density of $5\times10^3$ cells/well in 96-well plates and allowed to grow for 24 h. Thereafter, the cells were subjected to a 24-h serum starvation period, followed by incubation with varying doses of DMSO for 72 h. Next, the test reagent was added in compliance with the manufacturer's instructions. Using a Bio-Rad microplate reader, absorbance at 450 nm was measured in both treated and untreated cells. Assuming the absorbance in untreated cells indicates 100% cell viability, the percentage of absorbance in treated cells relative to that of untreated cells was calculated to determine cell viability.

*Immunoblot assays:* Immunoblot assays were conducted to detect the levels of α-SMA, fibronectin, and signaling proteins, as previously described [17]. After the indicated treatments, the cells were lysed, and proteins were separated using 10% SDS–PAGE and transferred onto polyvinylidene fluoride (PVDF) membranes. These were blocked for 1 h with

Table 1. Primers sequences.

| Gene | Nucleotide sequence (5′-3′) | Primer |
|---|---|---|
| GAPDH | ACTCCTCCACCTTTGACGCT | F |
| GAPDH | GGTCTCTCTCTTCCTCTTGTGC | R |
| IL-6 | TTCGGTCCAGTTGCCTTCT | F |
| IL-6 | GGTGAGTGGCTGTCTGTGTG | R |
| IL-8 | GGGTGGAAAGGTTTGGAGTAT | F |
| IL-8 | TAGGACAAGAGCCAGGAAGAA | R |
| Integrin α5 | GGGTGGCCTTCGGTTTA | F |
| Integrin α5 | GCTTTGCGAGTTGTTGAGAT | R |
| Integrin β1 | CCTACTTCTGCACGATG | F |
| Integrin β1 | TTTGCTACGGTTGGTTA | R |
| α-SMA | CCGACCGAATGCAGAAGGA | F |
| α-SMA | ACAGAGTATTTGCGCTCCGGA | R |
| Fibronectin | AATATCTCGGTGCCATTTGC | F |
| Fibronectin | AAAGGCATGAAGCACTCAAT | R |
| CTGF | GCGGCTTACCGACTGGA | F |
| CTGF | ACAGGCGGCTCTGCTTC | R |

F, forward; R, reverse.

fat-free milk and incubated for 2 h at room temperature or overnight at 4 °C with primary antibodies. Next, the protein bands were incubated with secondary antibodies and detected with ECL reagents. For the evaluation of protein levels and the normalization of target proteins to GAPDH, we used Image J software.

*Fluorescence microscopy:* Actin stress fiber formation was observed using fluorescence microscopy. HTFs were seeded into 35-mm dishes at a density of $3\times10^5$ cells/dish (three slides per container) and incubated in 10% FBS-DMEM for 1 day. Thereafter, the cells were subjected to a 24-h serum deprivation period. After being pretreated with SFN (10 μM), the cells were incubated with TGF-β (5 ng/ml) for 24 h. After 15 min of fixation with 4% paraformaldehyde and blocking with 1% BSA, we performed rhodamine-phalloidin (100 nmol/l in 1% BSA in phosphate buffer solution [1X PBS]) staining to detect F-actin. Next, after 10 min of DAPI staining, the cells were analyzed using a fluorescence microscope (ZEISS Axio Scope A1). The intensity of the fluorescence was evaluated using Image J [18].

*RT-qPCR:* The mRNA of integrins, cytokines, and growth factors in HTFs was measured by qRT-PCR. Serum-deprived cells were pretreated with SFN (10 μM), followed by TGF-β (5 ng/ml) for 24 h in the same medium. Total RNA was isolated from the cells using the RNAprep Pure Kit, and RT-qPCR was performed. The primer sequences for α-SMA, fibronectin, integrins, IL-6, IL-8, connective tissue growth factor (CTGF), and GAPDH are listed in Table 1, and the information pertaining to the exon–intron boundary is provided in Table 2. cDNA synthesis and RT-qPCR were conducted as previously described [17,19]. The RT-qPCR protocol used was as follows: 95°C for 3 min for primary denaturation, 95°C for 15 s for denaturation, 61°C for 15 s for annealing, and 72°C for 15 s for extension. A total of 40 cycles were conducted for each reaction. The relative protein expressions were normalized by the GAPDH expression level with the CT method used to calculate target change=$2^{-\Delta\Delta CT}$. All experiments were performed in triplicate, and the average value was calculated.

*Statistical analyses:* All results are expressed as mean ± standard deviation (SD). SPSS software was used to analyze the data. One-way ANOVAs and least significant difference (LSD) tests were used to compare the different groups. A p-value of $<0.05$ was used to infer significant differences. We performed all experiments in triplicate and repeated them at least three times.

## RESULTS

*SFN prevents TGF-β-induced contraction of HTFs.:* To assess the protective effects of SFN on the contractility of HTFs, cells cultured in a collagen gel were treated with the vehicle DMSO, TGF-β, and/or SFN (0.3 to 10 μM) for 3 days. Consistent with previous results, we observed the contraction of HTF-containing gels after TGF-β addition. This TGF-β-stimulated gel contraction was abolished in cells treated with SFN in a dose-dependent pattern (Figure 1A). Furthermore, we detected a time-dependent inhibition of SFN (10 μM) on TGF-β-stimulated gel contraction (Figure 1B). The compound SFN was dissolved in DMSO, with the

Table 2. Exon-intron boundary.

| Gene | Exon-intron | Intron-exon |
|---|---|---|
| GAPDH | 5′-CCTCCAAGGA^GTAAGACCCC-3′ | 5′-CTCCTCACAG^TTGCCATGTA-3′ |
| IL-6 | 5′-GTTAATTTAT^GTAAGTCATA-3′ | 5′-CCTGCCCCAG^TACCCCCAGG-3′ |
| IL-8 | 5′-TCACTGTGAG^GTAAGATGGT-3′ | 5′-CTTCACACAG^AGCTGCAGAA-3′ |
| Integrin α5 | 5′-CAGAATGTGG^GTGAGGGTGG-3′ | 5′-GGACACTAAG^AAAACCATCC-3′ |
| Integrin β1 | 5′-CGTTCCGAAC^GTGAGGGTCG-3′ | 5′-CTTAAAAAAG^AAGGGTTGCC-3′ |
| α-SMA | 5′-GTTCTATCGG^GTACTTCAGG-3′ | 5′-CTCATTGTAG^AAAGAGTGGT-3′ |
| Fibronectin | 5′-CCGAATGTAG^GTGAGGAAAT-3′ | 5′-ATTCATCTAG^ATGGTGCCAT-3′ |
| CTGF | 5′-ACAGGAAGAT^GTACGGAGAC-3′ | 5′-CCTCCTGCAG^GCTAGAGAAG-3′ |

concentration of DMSO in a 10 µM SFN solution being 0.1%. This vehicle alone, at the concentrations used, had no effect on the viability (Figure 1C) or contraction of HTFs (Figure 1D). All results were derived from three independent experiments (n=3).

*SFN inhibits α-SMA and fibronectin expression in TGF-β-treated HTFs:* To clarify whether SFN could impair the trans-differentiation of myofibroblasts stimulated with TGF-β, α-SMA and fibronectin expression were assessed. Stimulation with TGF-β (5 ng/mL) enhanced the expression of α-SMA and fibronectin in HTFs, while this effect was significantly suppressed by SFN in a dose-dependent manner (Figure 2A). The significant suppressive effect of SFN on α-SMA and fibronectin expression was supported by our densitometric analysis (Figure 2B). Additionally, RT-qPCR showed that TGF-β induced the upregulation of α-SMA and fibronectin mRNA levels. Similar to the immunoblot results, SFN suppressed the mRNA expression of the aforementioned molecules (Figure 2C). All values represent three independent experiments (n=3).

*SFN attenuates integrins α5 and β1 expression in HTFs:* To assess the effects of SFN on integrin expression, we cultured

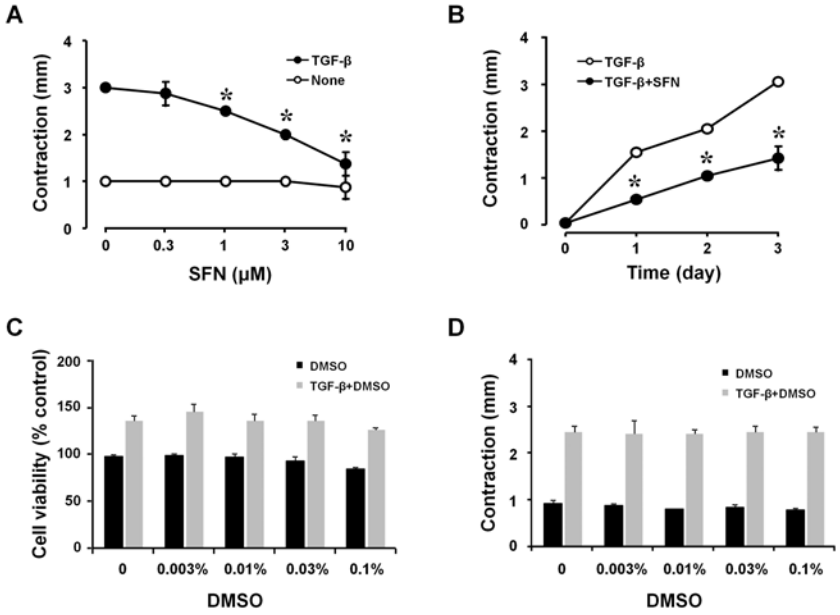


Figure 1. Effects of SFN on the contraction of collagen gels mediated by HTFs after TGF-β induction. **A**: HTFs embedded in collagen gels were treated with indicated concentrations of SFN (10 µM) or TGF-β (5 ng/ml) for 3 days. **B**: HTFs seeded in collagen gels were incubated with indicated treatment for different times, and gel contractions were measured. **C**: HTFs were subjected to treatment with varying concentrations of DMSO (0, 0.003%, 0.01%, 0.03%, and 0.1%) or TGF-β (5 ng/ml) for 72 h, and cell viability was assessed using a CCK-8 assay. (D) HTFs embedded in collagen gels were treated with the aforementioned concentrations of DMSO or TGF-β (5 ng/ml) for 3 days, with the extent of gel contraction being measured. Data are presented as mean ± SD (n=3). *p<0.05 compared to controls.

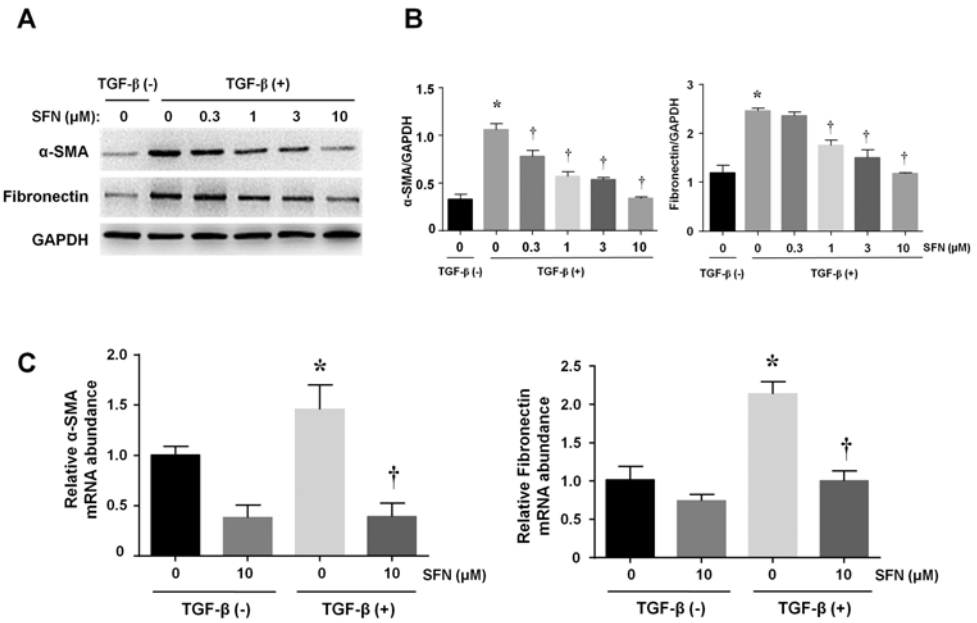


Figure 2. Effects of SFN on the expression of α-SMA and fibronectin in HTFs. **A**: Representative blots showing the expression of α-SMA and fibronectin. Densitometric analysis of α-SMA and fibronectin proteins normalized to GAPDH levels in (**A**) is shown in (**B**). **C**: Representative bar graphs showing the relative expression of α-SMA (left panel) and fibronectin (right panel) mRNAs in differentially treated cells. Data are presented as mean ± SD (n=3). *p<0.05 compared to controls. †p<0.05 compared to cells treated with TGF-β alone.

HTFs with TGF-β (5 ng/ml) and SFN (10 μM). After 24 h, the cells were collected, and RT-qPCR was performed. A significant increase in the expression of integrins α5 and β1 was observed in TGF-β-treated cells. This effect was inhibited by SFN administration (Figure 3). The values shown above are derived from three independent experiments (n=3).

*SFN inhibits the formation of stress fibers in HTFs:* Next, we examined the formation of stress fibers using immunofluorescent staining to assess the contractile activity of fibroblasts. Compared to controls, TGF-β-treated HTFs presented more stress fibers, while TGF-β-treated HTFs treated with SFN (10 μM) showed fewer stress fibers than the cells treated with only TGF-β (Figure 4). The inhibitory effect of SFN on the formation of stress fibers was confirmed by the analysis of fluorescence intensity (Figure 4B). The values shown above represent three independent experiments (n=3).

*SFN impairs the phosphorylation of MLC in HTFs:* We examined MLC phosphorylation in HTFs after a 24-h pretreatment with SFN (10 μM) followed by TGF-β (5 ng/ml) stimulation. HTFs were collected at different times, and the

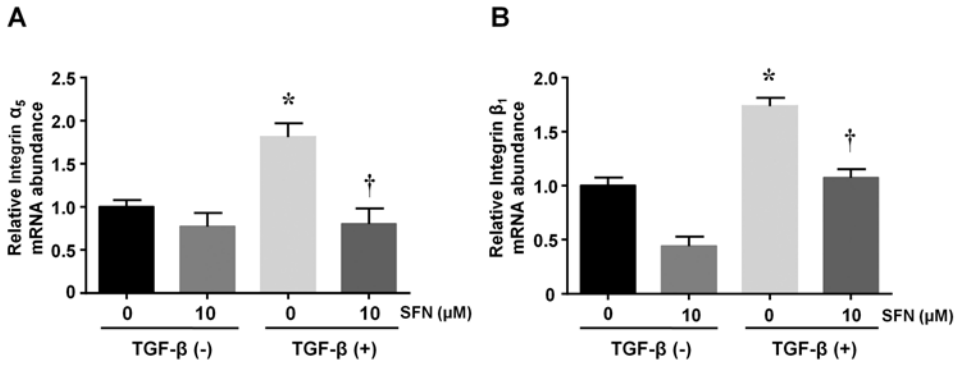


Figure 3. Effects of SFN on the expression of integrins in HTFs. Representative bar graphs showing the relative expression of integrins α5, β1 mRNA in differentially treated cells. Data are presented as mean ± SD (n=3). *p<0.05 compared to controls. †p<0.05 compared to cells treated with TGF-β alone.

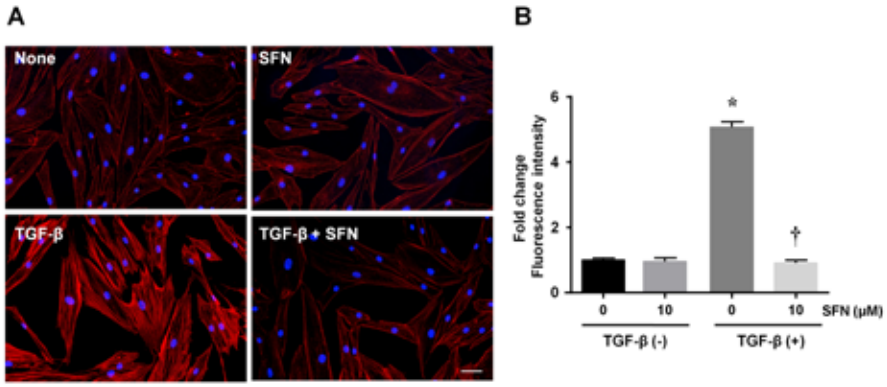


Figure 4. SFN suppresses the formation of stress fibers induced by TGF-β in HTFs. **A**: After embedding with collagen gels, cells were incubated for 24 h with or without SFN, followed by a 24 h culture with or without TGF-β. The formation of stress fibers was determined using Alexa Fluor 568–labeled phalloidin and DAPI staining. Scale bars: 50 μm. Fluorescence intensity analysis in (**A**) is shown in (**B**). Data are presented as mean ± SD (n=3). *p<0.05 compared to controls. †p<0.05 compared to cells treated with TGF-β alone.

phosphorylation of MLC was assessed with immunoblotting. The results showed that the phosphorylation of MLC was significantly enhanced after incubation with TGF-β (5 ng/ml), while treatment with SFN-impaired phosphorylation in a time-dependent manner (Figure 5A). Densitometric analysis showed that SFN significantly inhibited the phosphorylation of MLC after 2 h of TGF-β stimulation (Figure 5B). Thus, no changes in MLC phosphorylation were observed between the control and TGF-β + SFN-treated cells. The values shown above represent three independent experiments (n=3).

*SFN inhibits the activation of MAPK, AKT, Smad2/3 in TGF-β-treated HTFs:* To explore the possible mechanisms behind the inhibition of SFN on the transduction of TGF-β-associated pathways, we evaluated the expression of Smad2/3, AKT, ERK, and p38 MAPK. We observed a time-dependent activation of Smad2/3, AKT, ERK, and p38 MAPK in the

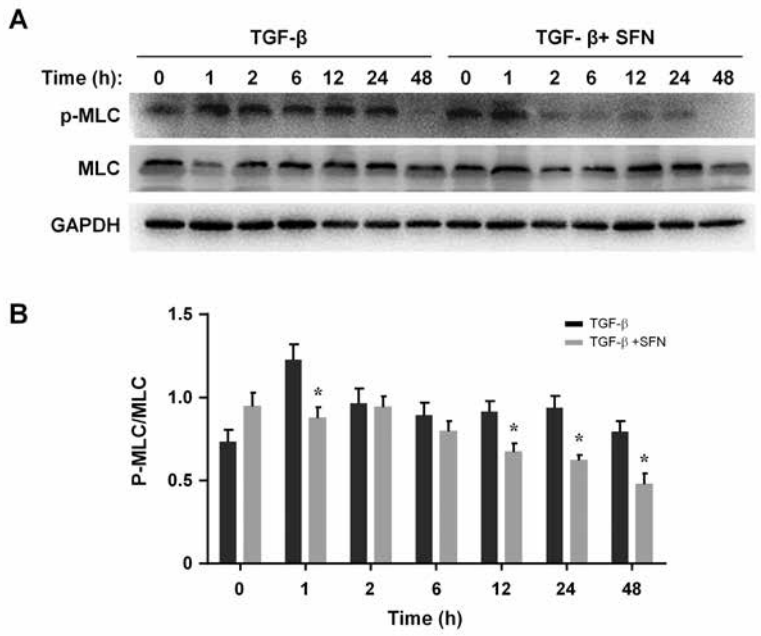


Figure 5. SFN suppresses TGF-β-induced MLC phosphorylation in HTFs. **A**: After a 24-h culture followed by a 24-h starvation, cells were incubated with or without SFN (10 μM) for an additional 24 h. Then, TGF-β (5 ng/ml) was added at indicated time points. Finally, total MLC and phospho-MLC were quantified. Densitometric analysis of p-MLC/MLC is presented in (**B**). Data are presented as mean ± SD (n=3). *p<0.05 compared to controls. †p<0.05 compared to cells treated with only TGF-β.

cells after TGF-β (5 ng/ml) induction (Figure 6A,C). TGF-β stimulation could effectively activate Smad2/3, ERK, and p38 MAPK after 1 h of treatment, and this activation was maintained for up to 24 h. Meanwhile, AKT was activated after 6 h of TGF-β addition and was maintained until 48 h. Conversely, SFN treatment inhibited the activation of Smad2/3 and ERK after 1 h of TGF-β stimulation, while AKT activation was impaired in SFN-treated cells at later time points (6 to 24 h). However, the phosphorylation of p-38 MAPK was not affected by SFN. These results indicate that SFN is significantly involved in TGF-β-associated activation of MAPK, AKT, and Smad2/3. Densitometric analysis confirmed the statistically significant effect of SFN on phosphorylation levels of Smad2/3, AKT, and ERK (Figure 6B,D–F). The values shown above represent three independent experiments (n=3).

*SFN suppresses TGF-β-induced expression of IL-6, IL-8, and CTGF in HTFs:* Finally, we evaluated the expression of inflammatory cytokines and growth factors to investigate the effects of SFN on the inflammation and growth of HTFs caused by TGF-β. The results showed that incubation with TGF-β significantly enhanced IL-6, IL-8, and CTGF expression compared to the controls. However, compared to cells incubated with TGF-β alone, SFN-treated cells exhibited significant impairment of IL-6, IL-8, and CTGF expressions. These results suggest that SFN suppressed TGF-β-induced inflammation and cell growth in HTFs (Figure 7). The values shown above represent three independent experiments (n=3).

## DISCUSSION

We explored the protective effects of SFN on TGF-β-caused fibrosis in HTFs. Mechanistic experiments revealed that SFN suppressed the trans-differentiation of HTFs into myofibroblasts and collagen contraction caused by TGF-β by impairing the production of fibronectin and α-SMA, as well as by inhibiting MLC, Smad2/3, MAPK, and ERK phosphorylation. These results indicate the participation of SFN in the suppression of classical and non-classical TGF-β pathways. Additionally, SFN inhibited the expression of integrins and several inflammatory factors.

Wound healing after glaucoma infiltration surgery can determine the outcome of the surgical procedure. The generation of filtering bleb scars after surgery results from local

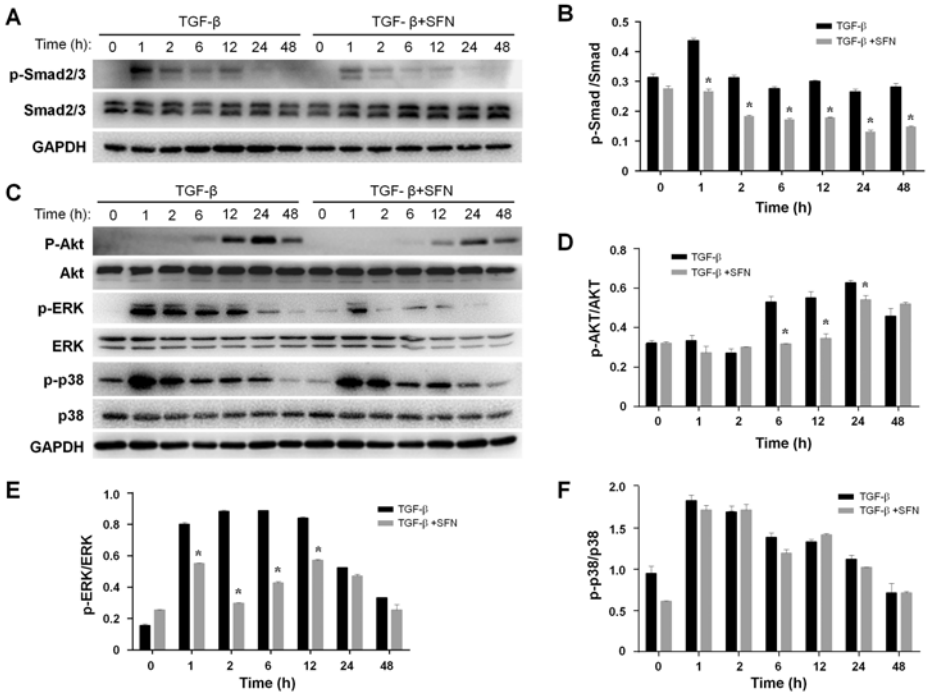


Figure 6. SFN suppresses TGF-β-induced Smad2/3, AKT, and MAPK activation in HTFs. **A**, **C**: After a 24-h culture followed by a 24-h starvation, cells were incubated with or without SFN (10 μM) for an additional 24 h. Then, TGF-β (5 ng/ml) was added at indicated time points. The protein levels of ERK, phospho-ERK, p38, phospho-p38, ATK, phospho-AKT, Smad2/3, and phospho-Smad2/3 were detected via western blot. Immunoblots resembling those in (**A**, **C**) were subjected to densitometric analysis to determine the intensity of the bands corresponding to phosphorylated Smad2/3 (**B**), AKT (**D**), ERK (**E**), or p38 (**F**). Data are presented as mean ± SD (n=3). *p<0.05 compared to controls. †p<0.05 compared to cells treated with only TGF-β.

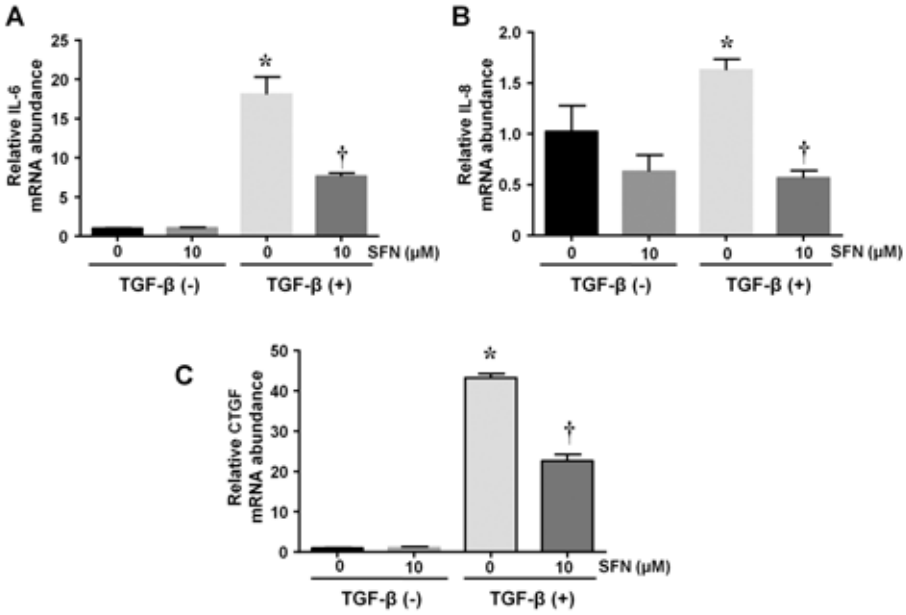


Figure 7. Effects of SFN on the mRNA expression of IL-6, IL-8, and CTGF induced by TGF-β in HTFs. Serum-deprived cells were first incubated with or without SFN (10 μM) for 24 h, followed by a 12-h treatment with TGF-β (5 ng/ml). Then, cells were collected, and the mRNA levels of IL-6, IL-8, and CTGF were determined. Data are presented as mean ± SD (n=3). *p<0.05 compared to untreated control cells. †p<0.05 compared to cells treated with TGF-β alone.

inflammation, such as the presence of CTGF and TGF-β, subconjunctival fibrosis characterized by excessive ECM (such as fibronectin and collagen) deposition and synthesis, cell differentiation, migration, and proliferation, as well as fibroblast proliferation [1]. Excessive ECM synthesis and conjunctival tissue contraction can contribute to scar formation during the bleb and ultimately result in surgery failure. Fibroblasts from the Tenon's capsule are known to play a key role in contractile scarring following glaucoma filtering surgery. The phenotypic transformation of fibroblasts into myofibroblasts and the expression of α-SMA are also significantly involved in wound healing.

Besides enhancing ECM production, myofibroblasts can lead to fibrosis. As regulatory factors and major components of ECM, abundant expressions of fibronectins participate significantly in scar formation caused by TGF-β after glaucoma surgery [20,21]. Here, we detected augmented fibronectin and α-SMA expression in TGF-β-treated HTFs, which was suppressed by SFN treatment, consistent with previous reports [22]. Furthermore, we verified the suppression of SFN in the contraction of collagen in vitro. The effects of SFN treatment on the trans-differentiation of fibroblasts have also been observed in other tissues [16,23], suggesting that SFN might serve as a general anti-fibrotic agent.

Due to their interaction with fibronectin and regulation of adhesion-dependent signaling [24], increased expressions of integrin α5 and β1 are significantly involved in myofibroblast differentiation induced by TGF-β [9], consistent with our results. Along with stress fiber formation and integrin α5 and β1 upregulation, fibronectin significantly promotes human corneal fibroblast-mediated collagen gel contraction [25]. Here, we showed that the upregulation of integrin α5 and β1 and fibronectin induced by TGF-β was inhibited by SFN, suggesting the participation of SFN in TGF-β-caused inhibition of collagen gel contraction. Contracting fibroblasts reorganize their cytoskeletal components and form actin stress fibers, leading to the generation of the tensile strength essential for postoperative scarring. The contractility of non-muscle cells is regulated by the phosphorylation of regulatory MLC [26]. It has been reported that TGF-β induces this phosphorylation, which increases in a time-dependent manner for at least 24 h [27,28]. Consistent with previous observations, we detected stress fiber formation and MLC phosphorylation in HTFs after TGF-β induction and showed the potential protection of SFN against the contraction caused by TGF-β. These results suggest that SFN inhibits the contractility of fibroblasts by reducing MLC activation, stress fiber formation, and fibronectin and integrin expression.

Non-canonical signaling pathways, such as MAPKs and AKT, and the canonical Smad2/3 pathway can be activated by TGF-β. In the canonical Smad2/3 pathway, the interaction of TGF-β with its receptors promotes the phosphorylation of Smad2/3, which subsequently interacts with Smad4 to generate a Smad2/3/4 complex that regulates the expression of ECM deposition- and myofibroblast differentiation-associated genes [24]. Additionally, the TGF-β-induced activation of ERK, p38 MAPK, and AKT pathways contributes to conjunctival fibrosis. Indeed, the inhibition of ERK and p38 MAPKs by U0126 can reduce the conversion of HTFs to myofibroblasts induced by TGF-β [29]. LY294002, an inhibitor of AKT signaling, can significantly reduce the proliferation and migration of conjunctival fibroblasts and α-SMA expression induced by TGF-β in these cells [30]. Our previous studies showed that inhibition of MAPK signaling by the ERK1/2 inhibitor PD98059 could significantly impair TGF-β–induced collagen gel contraction by HTFs, suggesting the importance of MAPKs in the effect of TGF-β [31]. Here, we show that SFN treatment impaired the activation of Smad2/3, AKT, and ERK1/2, suggesting the suppression of TGF-β-associated canonical and non-canonical pathways by SFN and its protective effect on TGF-β-induced HTF fibrogenesis.

Four phases can be identified during wound healing: hemostasis, inflammation, proliferation, and remodeling [4,5]. In the early stages after filtering surgery, greater infiltration of inflammatory cells is observed in surgical tissues. The presence of TGF, IL-6, IL-8, and CTGF [32] leads to the formation of postoperative filtering bleb scars. IL-8 is a chemoattractant of polymorphonuclear leukocytes. As a key stimulator and chemoattractant of lymphocytes [33], IL-6 is significantly connected to the core fibrotic process of trans-differentiation from Tenon's capsule fibroblasts to myofibroblasts [34,35]. Meanwhile, CTGF is an important pro-fibrosis factor and a downstream effector of TGF-β involved in several fibrotic diseases [36]. Here, we showed that SFN inhibited the expression of IL-6, IL-8, and CTGF induced by TGF-β. Additionally, previous studies have reported the protective effects of SFN against inflammation associated with myocardial fibrosis in diabetic cardiomyopathy [36], and pulmonary fibrosis induced by bleomycin in animal models [37]. Therefore, SFN also has the potential to impair the formation of scars through its anti-inflammatory activity.

In summary, we showed that SFN inhibited the contractility, trans-differentiation of myofibroblasts, and inflammation caused by TGF-β in HTFs through both canonical and non-canonical signaling pathways. Finally, SFN might be a multi-targeted therapeutic agent that prevents scar formation by inhibiting subconjunctival inflammation and fibrogenesis. To ascertain its relevance in clinical settings, its underlying mechanisms and potential for therapy need to be clarified in future research.

## ACKNOWLEDGMENTS

Funding: This study was supported by a grant (no. 81770889) from the National Science Foundation of China to Yang Liu and a grant from the Natural Science Foundation of Guangdong Province to Ye Liu (no. 2018A030313428). Declaration of interests. The authors declare no conflicts of interest. Dr. Ye Liu (liuye23@mail.sysu.edu.cn) and Dr. Hui Zheng (13926927853@139.com) are co-corresponding author for this paper.

## REFERENCES

1. Wei H, Lin L, Zhang X, Feng Z, Wang Y, You Y, Wang X, Hou Y. Effect of cytoglobin overexpression on extracellular matrix component synthesis in human tenon fibroblasts. Biol Res 2019; 52:23-[PMID: 30992080].
2. Grover DS, Kornmann HL, Fellman RL. Historical Considerations and Innovations in the Perioperative Use of Mitomycin C for Glaucoma Filtration Surgery and Bleb Revisions. J Glaucoma 2020; 29:226-35. [PMID: 31913225].
3. Yamanaka O, Kitano-Izutani A, Tomoyose K, Reinach PS. Pathobiology of wound healing after glaucoma filtration surgery. BMC Ophthalmol 2015; 15:157-165.
4. Wolters JEJ, van Mechelen RJS, Al Majidi R, Pinchuk L, Webers CAB, Beckers HJM, Gorgels TGMF. History, presence, and future of mitomycin C in glaucoma filtration surgery. Curr Opin Ophthalmol 2021; 32:148-59. [PMID: 33315724].
5. Zada M, Pattamatta U, White A. Modulation of Fibroblasts in Conjunctival Wound Healing. Ophthalmology 2018; 125:179-92. [PMID: 29079272].
6. Lin X, Yu M, Wu K, Yuan H, Zhong H. Effects of pirfenidone on proliferation, migration, and collagen contraction of human Tenon's fibroblasts in vitro. Invest Ophthalmol Vis Sci 2009; 50:3763-70. [PMID: 19264889].
7. Lockwood A, Brocchini S, Khaw PT. New developments in the pharmacological modulation of wound healing after glaucoma filtration surgery. Curr Opin Pharmacol 2013; 13:65-71. [PMID: 23153547].
8. Hu HH, Chen DQ, Wang YN, Feng YL, Cao G, Vaziri ND, Zhao YY. New insights into TGF-β/Smad signaling in tissue fibrosis. Chem Biol Interact 2018; 292:76-83. [PMID: 30017632].
9. Frangogiannis N. Transforming growth factor-β in tissue fibrosis. J Exp Med 2020; 217:e20190103[PMID: 32997468].
10. Li N, Cui J, Duan X, Chen H, Fan F. Suppression of type I collagen expression by miR-29b via PI3K, Akt, and Sp1

pathway in human Tenon's fibroblasts. Invest Ophthalmol Vis Sci 2012; 53:1670-8. [PMID: 22297492].

11. Cheng WS, Chen CL, Chen JT, Lin LT, Pao SI, Chen YH, Lu DW. AR12286 Alleviates TGF-β-Related Myofibroblast Transdifferentiation and Reduces Fibrosis after Glaucoma Filtration Surgery. Molecules 2020; 25:4422-41[PMID: 32993110].

12. Huang L, Ye Q, Lan C, Wang X, Zhu Y. AZD6738 Inhibits fibrotic response of conjunctival fibroblasts by regulating checkpoint kinase 1/*P53* and *PI3K*/*AKT* pathways. Front Pharmacol 2022; 13:990401[PMID: 36204234].

13. Houghton CA, Fassett RG, Coombes JS. Sulforaphane and Other Nutrigenomic Nrf2 Activators: Can the Clinician's Expectation Be Matched by the Reality? Oxid Med Cell Longev 2016; 2016:7857186[PMID: 26881038].

14. Tarozzi A, Angeloni C, Malaguti M, Morroni F, Hrelia S, Hrelia P. Sulforaphane as a potential protective phytochemical against neurodegenerative diseases. Oxid Med Cell Longev 2013; 2013:415078[PMID: 23983898].

15. Wu J, Han J, Hou B, Deng C, Wu H, Shen L. Sulforaphane inhibits TGF-β-induced epithelial-mesenchymal transition of hepatocellular carcinoma cells via the reactive oxygen species-dependent pathway. Oncol Rep 2016; 35:2977-83. [PMID: 26935987].

16. Kyung SY, Kim DY, Yoon JY, Son ES, Kim YJ, Park JW, Jeong SH. Sulforaphane attenuates pulmonary fibrosis by inhibiting the epithelial-mesenchymal transition. BMC Pharmacol Toxicol 2018; 19:13-[PMID: 29609658].

17. Liu Y, Kimura K, Orita T, Teranishi S, Suzuki K, Sonoda KH. All-trans-retinoic acid inhibition of transforming growth factor-β-induced collagen gel contraction mediated by human Tenon fibroblasts: role of matrix metalloproteinases. Br J Ophthalmol 2015; 99:561-5. [PMID: 25614514].

18. Nie Z, Li Y, Li X, Xu Y, Yang G, Ke M, Qu X, Qin Y, Tan J, Fan Y, Zhu C. Layer-by-Layer Assembly of a Polysaccharide "Armor" on the Cell Surface Enabling the Prophylaxis of Virus Infection. ACS Appl Mater Interfaces 2022; in press[PMID: 35639584].

19. Guo ZH, Liu PP, Wang H, Yang XX, Yang CC, Zheng H, Tang D, Liu Y. Inhibitory effects of luteolin on TLR3-mediated inflammation caused by TAK/NF-κB signaling in human corneal fibroblasts. Int J Ophthalmol 2022; 15:371-9. [PMID: 35310053].

20. Meyer-Ter-Vehn T, Grehn F, Schlunck G. Localization of TGF-β type II receptor and ED-A fibronectin in normal conjunctiva and failed filtering blebs. Mol Vis 2008; 14:136-41. [PMID: 18334936].

21. Välimäki J, Uusitalo H. Immunohistochemical analysis of extracellular matrix bleb capsules of functioning and non-functioning glaucoma drainage implants. Acta Ophthalmol 2014; 92:524-8. [PMID: 24020946].

22. Liu HR, Xia ZY, Wang NL. Sulforaphane modulates TGFβ2-induced conjunctival fibroblasts activation and fibrosis by inhibiting PI3K/Akt signaling. Int J Ophthalmol 2020; 13:1505-11. [PMID: 33078098].

23. Sun C, Li S, Li D. Sulforaphane mitigates muscle fibrosis in mdx mice via Nrf2-mediated inhibition of TGF-β/Smad signaling. J Appl Physiol (1985) 2016; 120(4):377–90.

24. Pardali E, Sanchez-Duffhues G, Gomez-Puerto MC, Ten Dijke P. TGF-β-Induced Endothelial-Mesenchymal Transition in Fibrotic Diseases. Int J Mol Sci 2017; 18:2157-79[PMID: 29039786].

25. Liu Y, Yanai R, Lu Y, Kimura K, Nishida T. Promotion by fibronectin of collagen gel contraction mediated by human corneal fibroblasts. Exp Eye Res 2006; 83:1196-204. [PMID: 16914141].

26. Peterson LJ, Rajfur Z, Maddox AS, Freel CD, Chen Y, Edlund M, Otey C, Burridge K. Simultaneous stretching and contraction of stress fibers in vivo. Mol Biol Cell 2004; 15:3497-508. [PMID: 15133124].

27. Ji Y, Lisabeth EM, Neubig RR. Transforming Growth Factor $\beta$1 Increases Expression of Contractile Genes in Human Pulmonary Arterial Smooth Muscle Cells by Potentiating Sphingosine-1-Phosphate Signaling. Mol Pharmacol 2021; 100:53-60. [PMID: 34031187].

28. Kimura K, Orita T, Fujitsu Y, Liu Y, Wakuta M, Morishige N, Suzuki K, Sonoda KH. Inhibition by female sex hormones of collagen gel contraction mediated by retinal pigment epithelial cells. Invest Ophthalmol Vis Sci 2014; 55:2621-30. [PMID: 24609629].

29. Wen J, Lin X, Gao W, Qu B, Ling Y, Liu R, Yu M. MEK inhibition prevents TGF-β1-induced myofibroblast transdifferentiation in human tenon fibroblasts. Mol Med Rep 2019; 19:468-76. [PMID: 30483803].

30. Liang L, Wang X, Zheng Y, Liu Y. All-trans-retinoic acid modulates TGF-β-induced apoptosis, proliferation, migration and extracellular matrix synthesis of conjunctival fibroblasts by inhibiting PI3K/AKT signaling. Mol Med Rep 2019; 20:2929-35. [PMID: 31322252].

31. Liu Y, Kimura K, Orita T, Teranishi S, Suzuki K, Sonoda KH. Inhibition by all-trans-retinoic acid of transforming growth factor-β-induced collagen gel contraction mediated by human tenon fibroblasts. Invest Ophthalmol Vis Sci 2014; 55:4199-205. [PMID: 24894398].

32. Futakuchi A, Inoue T, Wei FY, Inoue-Mochita M, Fujimoto T, Tomizawa K, Tanihara H. YAP/TAZ Are Essential for TGF-β2-Mediated Conjunctival Fibrosis. Invest Ophthalmol Vis Sci 2018; 59:3069-78. [PMID: 30025139].

33. Horn F, Henze C, Heidrich K. Interleukin-6 signal transduction and lymphocyte function. Immunobiology 2000; 202:151-67. [PMID: 10993289].

34. Seong GJ, Hong S, Jung SA, Lee JJ, Lim E, Kim SJ, Lee JH. TGF-β-induced interleukin-6 participates in transdifferentiation of human Tenon's fibroblasts to myofibroblasts. Mol Vis 2009; 15:2123-8. [PMID: 19862334].

35. Koh SW, Coll TJ, Rose L, Matsumoto Y, Higginbotham EJ. Antiglaucoma eye drop pulses–increased interleukin-6

secretion by Tenon's capsule fibroblast cultures. J Glaucoma 2004; 13:200-9. [PMID: 15118463].

36. Bao H, Jiang K, Meng K, Liu W, Liu P, Du Y, Wang D. TGF-β2 induces proliferation and inhibits apoptosis of human Tenon capsule fibroblast by miR-26 and its targeting of CTGF. Biomed Pharmacother 2018; 104:558-65. [PMID: 29800920].

37. Yan B, Ma Z, Shi S, Hu Y, Ma T, Rong G, Yang J. Sulforaphane prevents bleomycin-induced pulmonary fibrosis in mice by inhibiting oxidative stress via nuclear factor erythroid 2-related factor-2 activation. Mol Med Rep 2017; 15:4005-14. [PMID: 28487960].

Articles are provided courtesy of Emory University and the Zhongshan Ophthalmic Center, Sun Yat-sen University, P.R. China. The print version of this article was created on 6 November 2023. This reflects all typographical corrections and errata to the article through that date. Details of any changes may be found in the online version of the article.